Published in final edited form as:

Lancet. 2023 July 29; 402(10399): 397–410. doi:10.1016/S0140-6736(23)00775-4.

Compassionate Use of Genetically Engineered Pig Cardiac Xenotransplantation in a Human: What caused graft dysfunction?

Muhammad M Mohiuddin, MBBS[1,*,#], **Avneesh K Singh, PhD**[1], **Linda Scobie, PhD**[6,#], **Corbin E. Goerlich, MD**[1], **Alison Grazioli, MD**[2], **Kapil Saharia, MD**[3], **Claire Crossan, PhD**[6], **Allen Burke, MD**[4,#], **Cinthia Drachenberg, MD**[4,#], **Cihan Oguz, PhD**[5], **Tianshu Zhang, MD**[1], **Billeta Lewis, MS**[1], **Alena Hershfeld, MS**[1], **Faith Sentz**[1], **Ivan Tatarov, DVM**[1], **Sarah Mudd, RN**[1], **Gheorghe Braileanu, DVM**[1], **Kathryn Rice, MD**[4], **John F. Paolini, MD**[7], **Kent Bondensgaard, PhD**[7], **Todd Vaught, MS**[8], **Kasinath Kuravi, PhD**[8], **Lori Sorrells, BS**[8], **Amy Dandro, MS**[8], **David Ayares, PhD**[8], **Christine Lau, MD**[1,#], **Bartley P Griffith, MD**[1,#]

[1]Program in Cardiac Xenotransplantation, Department of Surgery, University of Maryland School of Medicine (UMSOM), Baltimore, MD 21201-1116

[2]Cardiac Surgery Intensive Care Unit, University of Maryland Medical Center (UMMC) Baltimore, MD 21201-1116

[3]Institute of Human Virology, Division of Infectious Disease, University of Maryland School of Medicine, Baltimore, MD 21201

[4]Department of Pathology, University of Maryland Medical Center (UMMC) Baltimore, MD 21201

[5]Integrated Data Sciences Section, Research Technologies Branch, National Institute of Allergy and Infectious Diseases, National Institutes of Health, Bethesda, MD 20892, USA

[6]Department of Biological and Biomedical Sciences, Glasgow Caledonian University, Greater Glasgow

[7]Kiniksa Pharmaceuticals Limited

[*]**Address correspondence to: Muhammad M Mohiuddin MBBS (MD), D.Sc. (Hon)** Professor of Surgery, Director, Program in Cardiac Xenotransplantation, University of Maryland School of Medicine, 10 S. Pine Street, MSTF 434B, Baltimore, MD 21201, MMOHIUDDIN@som.umaryland.edu.

[#]Full Professors

Authors contribution:

MMM wrote the paper, coordinated with other authors in collecting and analyzing data, assembled the requirements of the manuscript, and is the corresponding author. MMM and BPG designed the study. BPG, AKS, CG, AG, KS, DA, and CL collected data, edited, and provided their input on the paper. LS, AB, CD, CO, JFP, KB, TV, KK, LS, and AD, wrote specific sections of the manuscript, provided figures, and contributed to the discussion. BL, TZ, AH, FS, KR, GB, and SM helped generate the data.

Conflict of Interest:

DA, AD, TV, LS, and KK are employees of Revivicor, Inc, a subsidy of United Therapeutics, Inc. JPL and KB are employee of Kiniksa Pharmaceuticals. Members of Program in Cardiac Xenotransplantation received research funding from United Therapeutics, Inc.

Ethics approval:

This study received ethical approval from University of Maryland School of Medicine ethics department.

[8]Revivicor Inc, Blacksburg, VA

Abstract

Background: A genetically engineered (GE) pig cardiac xenotransplantation was performed in a non-ambulatory patient with end-stage heart failure and on extracorporeal membrane oxygenation (ECMO) support who was determined to be ineligible for an allograft. This report details our current understanding of factors important to the xenotransplantation outcome.

Methods: Extensive clinical monitoring in the ICU collected physiologic and biochemical parameters critical for the care of all heart transplant recipients. To ascertain the cause of xenograft dysfunction, we performed extensive histopathological studies, including electron microscopy and quantification of porcine cytomegalovirus/porcine roseolovirus (PCMV/PRV) in xenograft, recipient cells, and tissue by DNA PCR and RNA transcription. IVIG binding to donor cells and single-cell RNA sequencing (scRNASeq) of peripheral blood mononuclear cells was performed.

Findings: After successful xenotransplantation, the graft functioned well on echocardiography and sustained cardiovascular and other organ systems functions until the postoperative day (POD) 47 when diastolic heart failure occurred. At POD 50, the endomyocardial biopsy (EMB) revealed damaged capillaries with interstitial edema, red cell extravasation, rare thrombotic microangiopathy, and complement deposition. Increased anti-pig xenoantibodies, mainly IgG, were detected after IVIG administration for hypogammaglobulinemia and during the first plasma exchange. EMB on POD 56 demonstrated fibrotic changes consistent with progressive myocardial stiffness. Microbial cell-free DNA (mcfDNA) testing indicated increasing titers of PCMV/PRV cfDNA. Post-mortem sc-RNA-seq demonstrated overlapping etiologies.

Interpretations: Hyperacute rejection was avoided. We identified potential mediators of the observed endothelial injury. First, widespread endothelial injury indicates antibody-mediated rejection , Second, IVIG bound strongly to donor endothelium, possibly causing immune activation. Finally, reactivation and replication of latent PCMV/PRV in the xenograft possibly initiated a damaging inflammatory response. The critical knowledge gained points to specific measures to improve xenotransplant outcomes in the future.

Funding: Revivicor, Inc provided the pigs, and Kiniksa Pharmaceuticals provided anti-CD40 antibodies in kind. The University of Maryland School of Medicine and the University of Maryland Medical Center supported the remaining costs.

Introduction:

The first genetically engineered (GE) pig heart transplant into a human was the culmination of our three decades of research. We previously showed the longest survival of both heterotopic and orthotopic GE pig heart transplants in baboons(1–3). The clinical course leading to the recipient's death has been described earlier(4). Most notably, the recipient experienced a rapid onset of diastolic failure and global pathologic myocardial thickening of the xenograft. Here we describe three potential etiologies of xenograft endothelial cell (EC) damage: 1) Endogenous xenoantibody-mediated rejection (AMR), 2) exogenous administration of IVIG-containing xenoantibodies, and 3) reactivation of porcine cytomegalovirus/porcine roseolovirus (PCMV/PRV) within the xenograft.

Materials and Methods:

Xenograft Recipient:

The patient was a 57-year-old man with hypertension, chronic mild thrombocytopenia, nonischemic cardiomyopathy, and prior mitral valve repair who was hospitalized with severe heart failure. He had a left ventricular ejection fraction (LVEF) of 10% and was placed on veno-arterial extracorporeal membrane oxygenation (VA-ECMO). The patient received the highest level of care to the point of consideration of allotransplantation and mechanical support. Eligibility for both was denied mainly due to non-compliance and refractory ventricular tachycardia and eventually consented to xenotransplantation(4). Acceptable low levels of preformed anti-pig antibody (IgG and IgM) compared to a positive control (sensitized serum from baboons after pig xenograft rejection) and low levels of complement-dependent cytotoxicity (CDC) against clonally matched 10 gene-edited PAECs were determined as previously reported(1, 4, 5) (Fig S1 (i.&ii)). The immunobiology and clinical use of genetically-modified pigs for human transplantation have been described elsewhere(6).

Compassionate Use or Expanded Access

Sometimes called “compassionate use,” expanded access is a potential pathway for a patient with a serious or immediately life-threatening disease or condition to gain access to an investigational medical product (drug, biologic, or medical device) for treatment outside of clinical trials when no comparable or satisfactory alternative therapy options are available. (Language from FDA document)

Verification of Gene Modifications and Health Status of Pig:

The pig (A328.1) was produced by somatic cell nuclear transfer(7), which was clonally derived from fibroblasts that included ten gene edits (Table S1)(4) and were confirmed using flow cytometry and western blot analysis (7). Routine surveillance testing of the source animal was negative for all pathogens, with the exception of porcine endogenous retrovirus (PERV) A and B and porcine circovirus (PCV). Post-mortem detection of anti-PCMV antibodies by a western blot: PCMV glycoprotein B antigen (GenBank FJ595497.1; 2305–2574bp) was cloned, expressed, and purified from an *E.Coli* 10X Histag vector (Origene). PCMV antigen was probed with pig sera or antibodies as described using a western blot system (Simple Wes, Bio-techne).

Immunosuppression (IS):

The induction and maintenance IS regimen used successfully in our NHP studies was altered because of patient co-morbidities (Table 1, Supp Table 2)(1, 3, 4, 8–11) Primatized anti-CD40 mAb (clone 2C10R4) showed significantly prolonged islet allograft and cardiac xenograft survival in non-human primate models of transplantation(1, 3, 9, 11–15). Therefore, we used KPL-404, a humanized IgG4 monoclonal antibody engineered to bind CD40 and interfere with downstream T cell–dependent B cell–immune responses without triggering Fc effector functions. A pharmacokinetic-guided dosing paradigm was used to assess the adequacy of KPL-404 administration. Adjustments to the dosing regimen were

required, and a putative trough concentration of 150 ug/ml was constructed based on previous studies(16, 17).

Anti-Viral Prophylaxis and Treatment:

Ganciclovir 5 mg/kg q24hr was initially started for anti-viral prophylaxis. Due to leukopenia, ganciclovir dose was reduced to 2.5 mg/kg q24hr on day 16 and then converted to valacyclovir on day 19 (Table 1) as our recipient was CMV IgG negative. Ganciclovir was restarted on day 30 at 2.5 mg/kg q24hr and continued until POD 43 when rising PCMV/PRV microbial cf-DNA titers prompted a change to cidofovir (5mg/kg/day).

Cardiac Xenograft function and Immune Monitoring:

Longitudinal noninvasive imaging with weekly transthoracic echocardiograms (TTEs) and global longitudinal strain (GLS) was performed over 2 months to evaluate the xenograft function(18). Immune phenotyping for T and B cells to identify different subpopulations was done by immunostaining using flow cytometry techniques(1, 13). Post-mortem serum cytokines levels were measured by Biolegend LEGENDplex assay(1). IVIG binding and CDC were determined to donor porcine aortic endothelial cells (PAEC)(1, 4). Anti-pig non-gal antibody binding was measured in patient serum samples(1–4).

Histological Evaluation of Endomyocardial Biopsies and Explanted Xenograft:

Paraffin-embedded sections from multiple biopsies and sections of the explanted xenograft were stained with hematoxylin and eosin. Sections were analyzed semi-quantitatively for hemorrhage, necrosis, thrombosis, and cellular infiltrates. Immunostaining for immunoglobulins (IgG & IgM) and complement (C3d & C4d) was performed(1). For electron microscopy (EM), the samples were routinely processed and stained as previously described(19).

Single-Cell RNA Sequence (scRNASeq) Analysis:

10x Genomics Single Cell Chromium 5’ antibody-derived tag (ADT) and mRNA libraries were sequenced in two runs with a total yield of ~2.5 billion reads. The overall sequencing quality was high, with at least 94% of bases in the barcode regions having Q30 or above.

Using Cell Ranger and the GRCh38 transcriptome reference, the fastq files and raw count matrices were generated. The remainder of the analysis was performed using the Seurat package of R to remove the low-quality cells and log-normalize and integrate the pre-transplant and post-transplant samples. After the quality-based filtering, we obtained 15,895 cells with less than 10% mitochondrial gene expression and 171–3999 detected genes per cell. We used the R package Azimuth for annotating the cells using the human PBMC reference.

Differential expression analysis was performed on the log-normalized RNA expression data using MAST, whereas the enrichment profiles were generated using WebGestalt. The figures were generated using the R packages ggpubr, patchwork, scCustomize, and clusterProfiler. The single-sample GSEA (ssGSEA) analysis was performed using the R package Escape.

Statistical Analysis:

All statistical analysis and graph tabulation was performed on GraphPad Prism 8 (San Diego, CA), including Kaplan Meyer curves and line graph plots. For RNA seq, the p-values reported in the boxplots were computed using the Wilcoxon rank sum test.

Funding Source: Revivicor, Inc provided the pigs, and Kiniksa Pharmaceuticals Limited provided anti-CD40 antibodies in kind. The University of Maryland School of Medicine and the University of Maryland Medical Center supported the remaining costs.

Results:

Verification of Engineered Genes in Pig:

Selected gene deletion and the addition of human transgenes to the donor were confirmed (Fig. 1 (i) A, B & C) and re-verified after the explant of xenograft. There was some loss of CD47, HO1, CD46, and DAF transgene expression, and increased expression of the hTBM and hEPCR genes was identified (Fig. 1(ii)).

Immunosuppression Management:

The clinical course has been extensively reviewed elsewhere(4). Although we used a lower IS dose than the standard NHP regimen(1, 3, 4, 20), it was enough to deplete peripheral B and T lymphocytes. However, a lymph node extracted on POD 2 showed the presence of both B and T cells, indicating that depletion was incomplete (Fig. 2(i)). An extra dose of Rituxan was given after this evaluation. MMF therapy was stopped due to pancytopenia from POD 20–50 but was restarted after that as rejection was suspected. The patient was maintained on tacrolimus from days 20 to 54. Clearance of KPL-404 was higher than that predicted from healthy participant PK profiles. Blood loss, crystalloid repletion, ECMO, continuous renal replacement therapy, exudative effusions, high-dose IVIG, and plasmapheresis altogether likely confounded reaching the target trough. Turnaround time for levels was 24–48 hours. Interval doses were administered to compensate (Fig. 2 (ii)).

Immune Phenotyping, Anti-Non-Gal Antibody Levels, and Serum Cytokine Analysis:

Peripheral B lymphocytes remained low throughout and re-emerged after POD 50 (Fig. 2 (iii& iv)). T lymphocytes were depleted effectively for the first 10 days but then re-populated. The ratio of CD4/CD8 began increasing around day 19, peaked at day 21, and then started to decline before increasing again around POD 50 (Fig 2(iii)). Anti-pig antibody levels in the patient's serum dropped with induction. They remained low until POD 47, when a sharp increase of IgG and, to a lesser extent, IgM occurred, which corresponded with IVIG administration (Fig 2(v)). Serum troponin I level increased postoperatively but returned to baseline by POD 24, then rose steadily after POD 34(4).

The serum concentrations of various cytokines are shown in figure 2(vi). Increased levels of IL-6 were observed, but TNFα levels were not increased in this patient as observed by others in NHP models with PCMV/PRV infection (21); Interferon-gamma (IFN-γ) increase, as observed here, has been associated with other inflammatory responses due to mediators like IVIG(22). Intracellular cytokine-secreting cells were analyzed (fig (2 (vii)), and no

change in TNFα producing cells were observed. Figure 2(viii) demonstrates the increasing levels of PCMV/PRV cfDNA in the patient's serum.

Histopathology:

The first endomyocardial biopsy (EMB) was delayed to POD 34 due to persistent thrombocytopenia. The EMB demonstrated mild interstitial edema. Some C3d, C4d, IgG, and IgM depositions were seen without evidence of endothelial damage (Fig 3(i)). EM demonstrated a normal capillary network. Only 1–2% of EC in capillaries had degenerative cytoplasmic changes. (Fig 3(v), A&B)

The second biopsy on POD 50 was prompted by the abrupt diastolic failure of the xenograft. EMB demonstrated significant interstitial edema with spindle-shaped cells (fibroblasts) and disorganized endothelium with extravasation of erythrocytes. C4d, IgG, and IgM depositions were noticed (Fig 3(ii)). EM showed that approximately 50% of the capillaries had a severe endothelial injury with EC necrosis and/or marked cytoplasmic swelling and areas of membrane fragmentation. There was surrounding interstitial edema and focal extravasation of red blood cells. The adjacent myocytes displayed degenerative changes, including cytoplasmic swelling, myofilament disarray, and focal myocyte necrosis (Fig 3(v) C).

Histopathology of POD 56 EMB showed ischemic myocyte necrosis in 40% of cells with fibrous interstitial expansion. Rare microthrombi and C4d, IgG, and IgM-positive EC (Fig 3(iii)). On EM, 80–85% of the capillaries were markedly abnormal. Capillaries had marked endothelial nuclear enlargement and cytoplasmic swelling. Some capillaries had areas of the denuded basal lamina, abnormal wall contour, or loss of continuity of the capillary wall. In the interstitial areas with reduced veins, there were randomly distributed cell fragments, medium electron-dense proteinaceous aggregates, randomly oriented collagen fiber bundles, and prominent interstitial edema. The adjacent myocytes often showed cytoplasmic swelling disarray of the myofilaments. Focal cell necrosis was also noted. (Fig 3(vi)A)

Post-mortem H&E demonstrated a similar pattern as the POD 56 EMB, with myocyte necrosis, collagen deposition in expanded interstitial spaces with apoptotic nuclear fragments, and deposition of both IgG and IgM in the remaining capillaries (Fig 3(iv)). The EM showed extensive damage to the capillary network, extensive EC lysis and fragmentation, and early fibrosis in most interstitial areas. Viral particles were not identified in any tissue compartment on electron microscopic examination (Fig 3(vi)B).

Evaluation of IVIG Binding to pig Endothelial Cells:

The patient was given high doses of IVIG twice, and where the 2nd dose on day 47 corresponds to significant patient worsening. Previously it was demonstrated that IVIG does not bind to triple knockout PAECs in vitro. However, the binding was never tested for 10 gene knockout cells(23). Post-mortem, strong binding to the donor PAECs was observed with three different lots of the same brand/manufacturer of IVIG (Fig 4(i)). Intriguingly, no CDC was observed when tested using donor PAECs (Fig 4(ii)).

Evaluation of Potential Virus-Mediated Graft Dysfunction:

Testing for mcf-DNA of various pathogens was previously described. It showed a progressive increase in cfDNA of PCMV/PRV (4), despite multiple negative PCMV/PCV PCR tests of the pig nasal swab pre-transplant. Post-mortem serological detection of anti-PCMV antibodies by western blot confirmed the presence of PCMV/PRV (Fig 1 (i) D & E. Figure 2(vi) demonstrates the kinetics of PCMV/PRV cf-DNA and total donor-derived cf-DNA in relation to anti-viral therapy modifications. The spleen of the pig (A328.1) was re-tested for pCMV/PRV DNA by qPCR and conventional PCR. The PCMV/PRV DNA level in the pig's spleen was extremely low by qPCR, with only 3.8 copies detected per 100 ng DNA but detectable nonetheless by sensitive methods. Retrospective analysis of the pig's organs pre-xenotransplant found negligible numbers of PCMV/PRV DNA (after adjustment to the cell copy number, $5.30*10^{-4}$, $1.79*10^{3}$ and $2.55*10^{-5}$ respectively) (Fig 5(i) and (ii)). Whereas on the recipient's PBMCs isolation at day 45, $2.26*10^{2}$ PCMV/PRV DNA copies per porcine cell were detected along with the RBCs. (Fig 5(i)).

Post-mortem, a full assessment of PCMV/PRV DNAemia, was carried out in the recipient and different parts of the xenograft. PCMV/PRV DNA and porcine cellular DNA were detected in all recipient organs. PCMV/PRV was detected in all xenograft sections (Fig 5(iii)). PCMV/PRV DNA copy ranged from $2.63*10^{1}$ copies per porcine cell, in the recipient's kidney, to $4.06*10^{4}$ copies per porcine cell, in the recipient's spleen (Fig 5(iii)&S2).

To determine if PCMV/PRV DNAemia detected represented an actively replicating virus, xenograft and patient samples from the autopsy were assessed by RT-qPCR for the presence of U41, U57, and U100 PCMV/PRV RNA transcripts. These genes are homologous with the HHV-6 genes U41 (DNA binding protein), U57 (major capsid protein), and U100 (envelope glycoprotein), with U41, expressed early in the viral life cycle and U57 and U100 expressed late in the viral life cycle. While transcription was detected for all three targets in the porcine heart post-xenotransplant (Figure 5(iv)), recipient tissues (liver, spleen, and kidney) were also assessed and were found to be negative for PCMV/PRV transcription. (Table S3).

Patient PBMCs were assayed for evidence of PERV integration by measuring the PERV to pig genome ratio in the patient PBMC'c, compared to the pig. No evidence of PERV integration was detected (Fig S3).

Use of scRNASeq Analysis to Determine the Causes of Graft Dysfunction

As shown in Figure 6(i), the most dominant changes in immune cell type composition across the time points were observed for monocytes, CD4+ T cells, CD8+ T cells, and NK cells. We further interrogated the data using GSEA and observed a significant increase (post- vs. pre-transplant) in the median gene set enrichment score (Fig 6(ii))(24) identified from the expression profiles of the 200 genes previously associated with allograft rejection (Fig 6(ii A)). A significant increase was also observed using the hallmark gene sets from the molecular signatures database(25) associated with the overall inflammatory response (Fig 6 (ii B)) and interferon alpha and gamma responses (Figures 6 (ii C-D). While the overall inflammatory response steadily increased over time, the kinetics were somewhat different

for the three other enrichment scores, wherein an increase after the IVIG treatment followed an initial drop. Supplementary Figure S4 (a-b) visualizes the average expression levels of the upregulated genes (by at least 50%) present in the hallmark allograft rejection signature.

Similar trends were observed in the gene set enrichment score distributions more directly linked to IVIG treatment shown in Fig 6 (ii E-H). The median NK-mediated cytotoxicity enrichment score steadily increased over time (Fig 6 (ii G)), whereas the overall leukocyte-mediated Fig 6 (ii F) and more specific T-cell mediated cytotoxicity (Fig 6 (ii H) enrichment scores first increased (POD 38 vs. Pre), then decreased (POD 52 vs. POD 38), which was followed by an increase upon IVIG treatment. Interestingly, T-cell-specific cytotoxicity showed a more significant change (POD 59 vs. POD 52) than the overall leukocyte-mediated cytotoxicity after IVIG treatment.

Our analysis of the genes upregulated by at least 50% (with FDR~0) after the transplant surgery resulted in an enrichment profile that included a set of pathways and a Gene Ontology (GO) term associated with B cell receptor (BCR) signaling (Fig 6(iii), S4 c-d).

A second set of biological pathways and GO terms enriched among the genes upregulated in the post-transplant samples was consistent with a viral infection, endothelial damage, and antigen presentation (Fig 6(iii), S4, e-f). This enrichment profile was specifically composed of elements such as viral myocarditis, antigen presentation, human cytomegalovirus infection, response to the virus, and leukocyte transendothelial migration, thereby providing potential mechanistic insights into the clinical events leading to POD 59.

Discussion:

The first successful cardiac xenograft from a 10-gene modified pig in a human sustained life despite the recipient’s preexisting conditions and multiple surgical and non-surgical complications until the patient died from graft failure on POD 60. The GE pig was cleared as a donor after testing with all available techniques for the presence of any pathogens and low anti-pig non-Gal antibodies consistent with our screening methods in NHP experiments. The patient stayed hemodynamically stable with excellent graft function for 47 days without needing any inotropes, abnormal chronotropic or ionotropic response to drugs or stress, and stable EKG. Then xenograft suddenly became edematous and lost diastolic function. EMB revealed an accumulation of fluid and red blood cells with limited inflammatory cells in the interstitial space. The interstitial edema was replaced by fibrotic tissue over the next few days. At this time, the patient’s condition rapidly deteriorated, support was withdrawn with the family’s consent, and the patient expired.

On histology and EM, the myocardial capillary bed and the surrounding myocardial cells demonstrated worsening EC injury over time associated with degenerative changes in the myocytes, including organelle and cytoplasmic swelling with disarray and loss of myofilaments. The exact cause of this damage cannot be clearly determined, but several possible reasons have been investigated as discussed below. A thorough examination of biopsies or post-mortem specimens found no intact virus or viral particle.

Due to pancytopenia and susceptibility to recurrent infections, the patient's IS had to be reduced from the proven successful levels in NHP models(1, 26). Significant B and T lymphocytes were present in the mediastinal lymph node after two days, indicating incomplete induction. B cell phenotyping reveals the presence of plasma cells as expected, but their phenotype analysis was not accurate due to very few circulating B cells. MMF is an essential component of the IS in non-NHP experiments[3,10,25]. MMF was stopped completely from POD 20–54 and may have contributed to xenoantibody-mediated EC damage. Tacrolimus was added instead of MMF and, Just like in NHP studies, proved ineffective in preventing rejection (27).

Our NHP studies demonstrated that a high dose of 2C10R4 was required to suppress B cell function effectively(28). The emergence of anti-graft antibodies was not seen as long as an effective anti-CD40 costimulatory blockade existed. The minimum efficacious dose of KPL-404 in humans in the complex transplant setting has not yet been determined. Thus, the goal in this patient was to deliver the highest concentration attainable, as appropriate from safety studies, accounting for extrinsic factors. It is possible that the elevated inflammatory response may have increased the amount of drug needed to maintain therapeutic levels in this patient (e.g., target-mediated drug disposition). It is also possible that extrinsic factors such as renal replacement therapy, exudative effusions, IVIG binding to EC preventing FC binding of the antibody, and plasmapheresis may have also reduced the bioavailability of this therapeutic antibody to its target.

The patient was administered exogenous IVIG because of severe hypogammaglobulinemia and due to overwhelming evidence of its beneficial effects in allotransplantation. Due to the suspicion that IVIG may have played a role, three different lots of commercially available IVIG were tested with PAECs from the heart (A328.1) and found to have a strong binding with PAECs. The complement-mediated cytotoxicity was not detected in vitro, perhaps due to the presence of constitutive expression of human complement regulatory genes in the pig organ. Though not tested, It is possible that non-complement-dependent inflammation, such as antibody-dependent cell cytotoxicity (ADCC), could have contributed to the destruction of EC. High levels of anti-pig IgG in the patient's serum and increased binding of anti-pig IgG and, to a lesser extent, IgM on IHC strongly suggest an exogenous source of IgG. The role of anti-pig antibodies in IVIG preparation and their role in endothelial damage may be more critical in xenotransplantation than allotransplantation and should be further evaluated.

Based on the pathological findings in other NHP xenotransplants and in the biopsies on this patient, the possibility of AMR is also to be considered. There is a definite endothelial injury in the first biopsy, as well as C4d deposition (though not impressive) in one biopsy and limited thrombi in the last biopsy. The illustrated findings are the features associated with AMR and could have resulted from reduced IS drug levels in the recipient. Expression of some transgene (HO1, CD47, CD46, and DAF) decreased, perhaps due to loss of EC. However, the loss of their protective function cannot be overruled. The EPCR and TBM expression increased post-mortem, likely in response to inflammation.

The critical role of complement in this study cannot be overlooked despite the presence of protective genes and C1 esterase inhibition. Limited complement assays were performed

due to insufficient tissue availability and proper controls. The assays performed may not be sensitive and specific enough to provide the correct interpretation of this major pathway's role, e.g., the autologous role of C3. A thorough evaluation will be undertaken in future experiments.

In defining the relevance and role of PCMV/PRV "transmission" in the recipient's worsening condition, we must be cautious using this terminology. From the morphological/pathological point of view, it is impossible to categorically attribute the damage solely to viral infection due to the absence of viral tissue replication in nuclei and the absence of viral cytopathic changes on light and electron microscopy. A xenograft with PCMV is analogous to a newborn pig infected with PCMV (i.e., immunologically naïve) in which setting PCMV can induce cardiac lesions. Initially, the detection of the virus did not constitute evidence of infection or transmission, given the nature of the assay used(4). Likewise, a previous report stating that a high level of TNFα was observed in the recipient is also incorrect(29), and it was not observed in the original study (4).

Numerous recent publications have commented on the sensitivity issues with donor testing (30–32). The diagnostic sensitivity and specificity of a PCR assay for PCMV/PRV are challenging as this can vary based on the age of the pig, the sample type submitted for testing, and the PCR assay utilized. The optimal sample type and PCR assay for latent PCMV/PRV are unknown. This limitation is clear because our qPCR assays detected PCMV in the pig, while the PCR assay for routine surveillance testing did not. Serological testing should be developed to detect latent viruses. The serology tests now available may be more accurate for a latent virus.

Our findings support the evidence that the pig was indeed positive for PCMV/PRV DNA which was also present in the transplanted xenograft. DNAemia was also detected in the tissues assessed, including the xenograft; however, transcription of the virus was not identified in any tissue from the recipient. No PCMV/PRV DNA was detected in the absence of porcine cell DNA, suggesting that PCMV/PRV DNAemia may have resulted from lysed or circulating xenograft cells or from PCMV/PRV virions generated in the xenograft, as opposed to the presence of replicating PCMV/PRV within the patient organs. Despite the evidence of viral DNAemia and PCMV/PRV RNA transcription by PCR assays, there was no evidence of cytopathic changes in the heart or evidence of viral presence on electron microscopy (EM). This would suggest that active replication-producing viral proteins is absent or below the detection limit using EM. The absence of lesions does not permit any comparison to disease in swine.

Reactivation of latent PCMV/PRV virus in the porcine heart, possibly due to immune suppression, could be potentially responsible for the initiation of dramatic endothelial injury due to cell lysis, as evidenced by the electron microscopy data. The ultrastructural evaluation of the myocardium demonstrated progressive damage and loss of the capillary bed. The etiology of this process is unclear, but the differential diagnosis includes immune-mediated and cytotoxic injury from exogenous and endogenous components. Cell injury with membrane and organelle damage can be seen in sepsis secondary to an inflammatory response syndrome

The evidence provided here through scRNASeq analysis confirms the difficulty of pinpointing any single etiology for the xenograft dysfunction and the complexities of a vulnerable patient in exacerbating the effect of three possible causes of endothelial damage. This enrichment profile was specifically composed of elements suggestive of viral myocarditis, antigen presentation, and leukocyte transendothelial migration, thereby providing potential mechanistic insights into the clinical events leading to POD 59 after the transplant surgery. Thus, it supports an inflammatory response from potential contributions of PCMV/PRV activation, AMR, and IVIG administration.

This experimental transplant was successful as the patient survived for 60 days, and the xenograft functioned well for the first 47 days. The immunosuppression used successfully in the NHP experiments could not be consistently applied in this patient due to his co-morbidities, including pancytopenia. It was unfortunate to discover that PCMV/PRV was present in the xenograft, and IVIG had to be given for severe hypogammaglobulinemia. In light of our findings above, both graft characteristics, e.g., activation of latent virus, and the recipient, e.g., immunocompromised state, may have played a role in graft dysfunction. This experience provides valuable lessons for future xenotransplantation: 1) we must avoid any opportunity for the potential latent virus in xenograft; 2) the use of IVIG and the reduction of IS may need strong justification, and every effort should be made to use the proven IS in NHP experiments; 3) proper determination of dosing and monitoring of co-stimulation blockade antibody; 4) tacrolimus alone has not shown efficacy in any xenotransplant trial and must be used with some caution; and 5) better patient selection with a relatively healthier patient who does not require ECMO support would be preferable.

We conclude that, except for a few unexpected complications, the GE pig heart and anti-CD40-based regimen could sustain a patient’s life for 60 days. More GE pigs to human transplants will facilitate a better understanding of the mechanism of xenograft failure in humans and help us better manage clinical xenotransplantation.

Supplementary Material

Refer to Web version on PubMed Central for supplementary material.

Acknowledgments

We want to thank our core laboratories, including the University of Maryland School of Medicine Center for Innovative Biomedical Resources (CIBR), which includes Veterinary Resources, Flow Cytometry Facility (FCC), Institute of Genomic Sciences (IGS), and the clinical staff of the University of Maryland Medical Center (UMMC) for their contribution to this case. Karius for providing mcfDNA monitoring. We want to thank Drs. Jonathan Bromberg, Valeria Mas, and Charles Hong for their critical evaluation of the manuscript, and Ms. Patricia Jackson for her administrative help.

Abbreviations:

ADCC	antibody-dependent cell cytotoxicity
AMR	Antibody-Mediated Rejection
CDC	Complement-Dependent Cytotoxicity

cfDNA	cell-free DNA
EM	Electron Microscopy
EMB	Endomyocardial Biopsy
ICU	Intensive Care Unit
mcf-DNA	microbial cell-free DNA
MMF	Mycophenolate Mofetil
NHP	Non-Human Primates
PAECs	porcine aortic endothelial cells
PCMV	Porcine Cytomegalovirus
PCV	Porcine Circovirus
PERV	Porcine Endogenous Retrovirus
POD	Postoperative Day
PRV	Porcine Roseolovirus
scRNASeq	single-cell RNA sequencing
TNF	Tumor Necrosis Factor
VA-ECMO	Veno-Arterial Extracorporeal Membrane Oxygenation

References:

1. Mohiuddin MM, Goerlich CE, Singh AK, Zhang T, Tatarov I, Lewis B, et al. Progressive genetic modifications of porcine cardiac xenografts extend survival to 9 months. Xenotransplantation. 2022:e12744. [PubMed: 35357044]
2. Mohiuddin MM, Singh AK, Corcoran PC, Azimzadeh AM, Ayares D, Hoyt RF, et al. B cell depletion by anti CD20 prolongs GalKO.hCD46 pig heterotopic cardiac xenograft survival in baboons. Xenotransplantation. 2009;16(5):357-.
3. Mohiuddin MM, Singh AK, Corcoran PC, Thomas ML 3rd, Clark T, Lewis BG, et al. Chimeric 2C10R4 anti-CD40 antibody therapy is critical for long-term survival of GTKO.hCD46.hTBM pig-to-primate cardiac xenograft. Nat Commun. 2016;7:11138. [PubMed: 27045379]
4. Griffith BP, Goerlich CE, Singh AK, Rothblatt M, Lau CL, Shah A, et al. Genetically Modified Porcine-to-Human Cardiac Xenotransplantation. N Engl J Med. 2022;387(1):35–44. [PubMed: 35731912]
5. Azimzadeh AM, Byrne GW, Ezzelarab M, Welty E, Braileanu G, Cheng X, et al. Development of a consensus protocol to quantify primate anti-non-Gal xenoreactive antibodies using pig aortic endothelial cells. Xenotransplantation. 2014;21(6):555–66. [PubMed: 25176173]
6. Goerlich CE, Singh AK, Griffith BP, Mohiuddin MM. The immunobiology and clinical use of genetically engineered porcine hearts for cardiac xenotransplantation. Nat Cardiovasc Res. 2022;1(8):715–26. [PubMed: 36895262]
7. Eyestone W. Gene-edited pigs for xenotransplantation2020.
8. Cooper DKC, Hara H, Iwase H, Banks CA, Cleveland DC. An approach to induction of tolerance to pig cardiac xenografts in neonates. Xenotransplantation. 2018;25(6):e12454.

9. Iwase H, Ekser B, Satyananda V, Bhama J, Hara H, Ezzelarab M, et al. Pig-to-baboon heterotopic heart transplantation--exploratory preliminary experience with pigs transgenic for human thrombomodulin and comparison of three costimulation blockade-based regimens. Xenotransplantation. 2015;22(3):211–20. [PubMed: 25847282]
10. Iwase H, Hara H, Ezzelarab M, Li T, Zhang Z, Gao B, et al. Immunological and physiological observations in baboons with life-supporting genetically engineered pig kidney grafts. Xenotransplantation. 2017;24(2).
11. Langin M, Mayr T, Reichart B, Michel S, Buchholz S, Guethoff S, et al. Consistent success in life-supporting porcine cardiac xenotransplantation. Nature. 2018;564(7736):430–3. [PubMed: 30518863]
12. Iwase H, Liu H, Wijkstrom M, Zhou H, Singh J, Hara H, et al. Pig kidney graft survival in a baboon for 136 days: longest life-supporting organ graft survival to date. Xenotransplantation. 2015;22(4):302–9. [PubMed: 26130164]
13. Mohiuddin MM, Singh AK, Corcoran PC, Hoyt RF, Thomas ML 3rd, Ayares D, et al. Genetically engineered pigs and target-specific immunomodulation provide significant graft survival and hope for clinical cardiac xenotransplantation. J Thorac Cardiovasc Surg. 2014;148(3):1106–13; discussion 13–4. [PubMed: 24998698]
14. Mohiuddin MM, Singh AK, Corcoran PC, Hoyt RF, Thomas ML 3rd, Lewis BG, et al. Role of anti-CD40 antibody-mediated costimulation blockade on non-Gal antibody production and heterotopic cardiac xenograft survival in a GTKO.hCD46Tg pig-to-baboon model. Xenotransplantation. 2014;21(1):35–45. [PubMed: 24164510]
15. Lowe M, Badell IR, Thompson P, Martin B, Leopardi F, Strobert E, et al. A novel monoclonal antibody to CD40 prolongs islet allograft survival. Am J Transplant. 2012;12(8):2079–87. [PubMed: 22845909]
16. Marken J, Muralidharan S, Giltiay NV. Anti-CD40 antibody KPL-404 inhibits T cell-mediated activation of B cells from healthy donors and autoimmune patients. Arthritis Res Ther. 2021;23(1):5. [PubMed: 33407802]
17. Samant M, Wheeler A, Jiang G, Njenga M, Spiers M, Pano A, Paolini J, Safety, Tolerability, Pharmacokinetics, Receptor Occupancy, and Suppression of T-cell-Dependent Antibody Response in a Phase 1 Study with KPL-404, an anti-CD40 Monoclonal Antibody. Arthritis Rheumatol. 2021.
18. Hong SN, Mohiuddin MM, Ananthram M, Soares C, Goerlich CE, Dickfeld TL, et al. Longitudinal Echocardiogram Imaging in the First Genetically Modified Porcine to Human Cardiac Xenotransplant. JACC Cardiovasc Imaging. 2023.
19. Drachenberg CB, Steinberger E, Hoehn-Saric E, Heffes A, Klassen DK, Bartlett ST, et al. Specificity of intertubular capillary changes: comparative ultrastructural studies in renal allografts and native kidneys. Ultrastruct Pathol. 1997;21(3):227–33. [PubMed: 9183823]
20. Goerlich CE, Griffith BP, Shah A, Treffalls JA, Zhang T, Lewis B, et al. A Standardized Approach to Orthotopic (Life-supporting) Porcine Cardiac Xenotransplantation in a Nonhuman Primate Model. Transplantation. 2023.
21. Fiebig U, Abicht JM, Mayr T, Langin M, Bahr A, Guethoff S, et al. Distribution of Porcine Cytomegalovirus in Infected Donor Pigs and in Baboon Recipients of Pig Heart Transplantation. Viruses. 2018;10(2).
22. Castro-Dopico T, Clatworthy MR. IgG and Fcgamma Receptors in Intestinal Immunity and Inflammation. Front Immunol. 2019;10:805. [PubMed: 31031776]
23. Yamamoto T, Cui Y, Patel D, Jagdale A, Iwase H, Ayares D, et al. Effect of intravenous immunoglobulin (IVIg) on primate complement-dependent cytotoxicity of genetically engineered pig cells: relevance to clinical xenotransplantation. Sci Rep. 2020;10(1):11747. [PubMed: 32678137]
24. Subramanian A, Tamayo P, Mootha VK, Mukherjee S, Ebert BL, Gillette MA, et al. Gene set enrichment analysis: a knowledge-based approach for interpreting genome-wide expression profiles. Proc Natl Acad Sci U S A. 2005;102(43):15545–50. [PubMed: 16199517]
25. Liberzon A, Birger C, Thorvaldsdottir H, Ghandi M, Mesirov JP, Tamayo P. The Molecular Signatures Database (MSigDB) hallmark gene set collection. Cell Syst. 2015;1(6):417–25. [PubMed: 26771021]

26. Goerlich CE, Griffith B, Singh AK, Abdullah M, Singireddy S, Kolesnik I, et al. Blood Cardioplegia Induction, Perfusion Storage and Graft Dysfunction in Cardiac Xenotransplantation. Front Immunol. 2021;12:667093.

27. Yamamoto T, Hara H, Foote J, Wang L, Li Q, Klein EC, et al. Life-Supporting Kidney Xenotransplantation from Genetically-Engineered Pigs in Baboons: A Comparison of Two Immunosuppressive Regimens. Transplantation. 2019.

28. Mohiuddin MM, Singh AK, Corcoran PC, Thomas ML, Eckhaus MA, Lewis B, et al. B Cell Depletion Along with Co-Stimulation Blockade by Anti CD40 (Clone 2C10) Extends Graft Survival Significantly in a Heterotopic Cardiac Xenotransplantation Model. Transplantation. 2012;94(10):70-. [PubMed: 22706321]

29. Denner J, Langin M, Reichart B, Kruger L, Fiebig U, Mokelke M, et al. Impact of porcine cytomegalovirus on long-term orthotopic cardiac xenotransplant survival. Sci Rep. 2020;10(1):17531. [PubMed: 33067513]

30. Halecker S, Hansen S, Krabben L, Ebner F, Kaufer B, Denner J. How, where and when to screen for porcine cytomegalovirus (PCMV) in donor pigs for xenotransplantation. Sci Rep. 2022;12(1):21545. [PubMed: 36513687]

31. Denner J. Virus Safety of Xenotransplantation. Viruses. 2022;14(9).

32. Mueller NJ, Denner J. Porcine cytomegalovirus/porcine roseolovirus (PCMV/PRV): A threat for xenotransplantation? Xenotransplantation. 2022;29(5):e12775. [PubMed: 36082418]

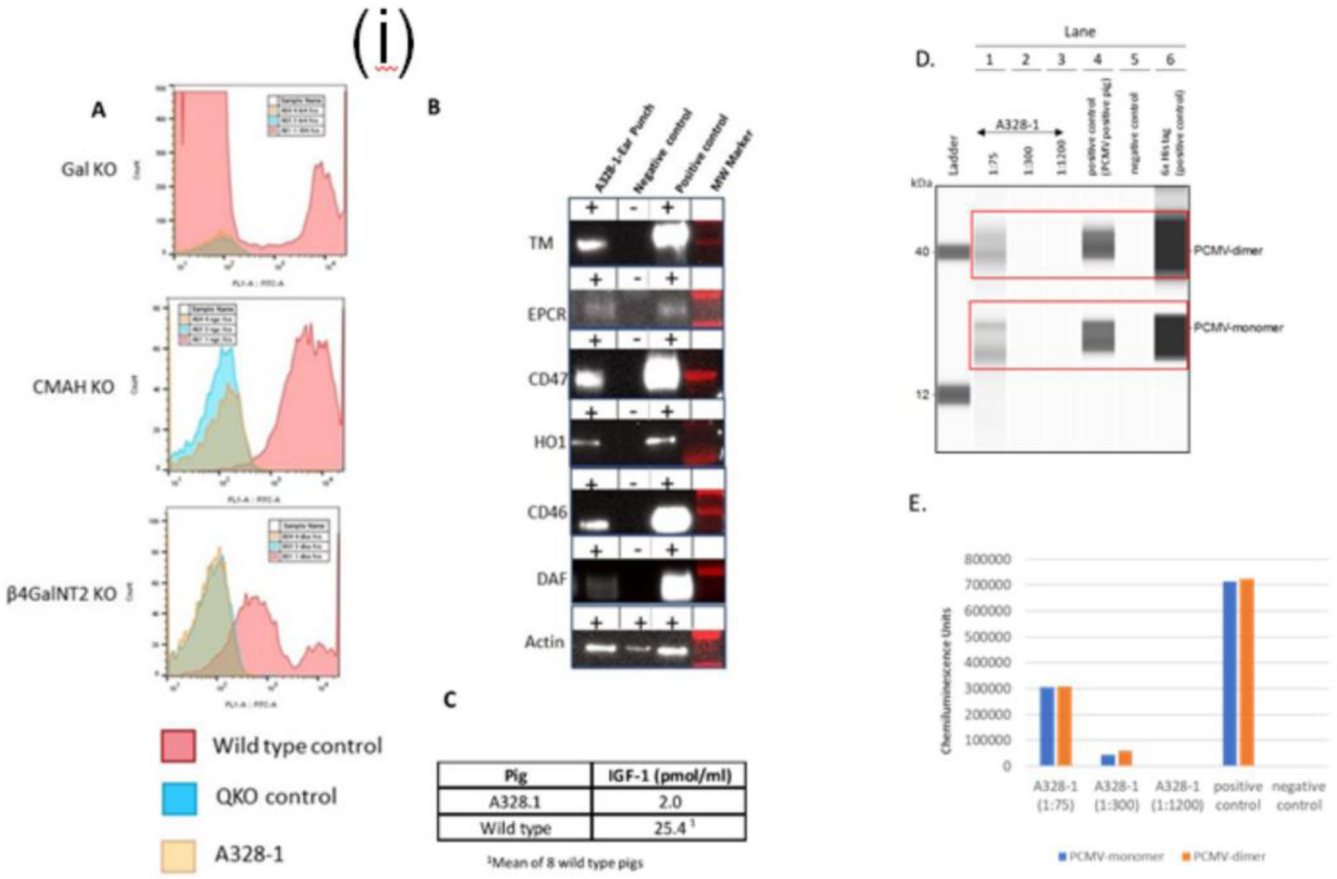

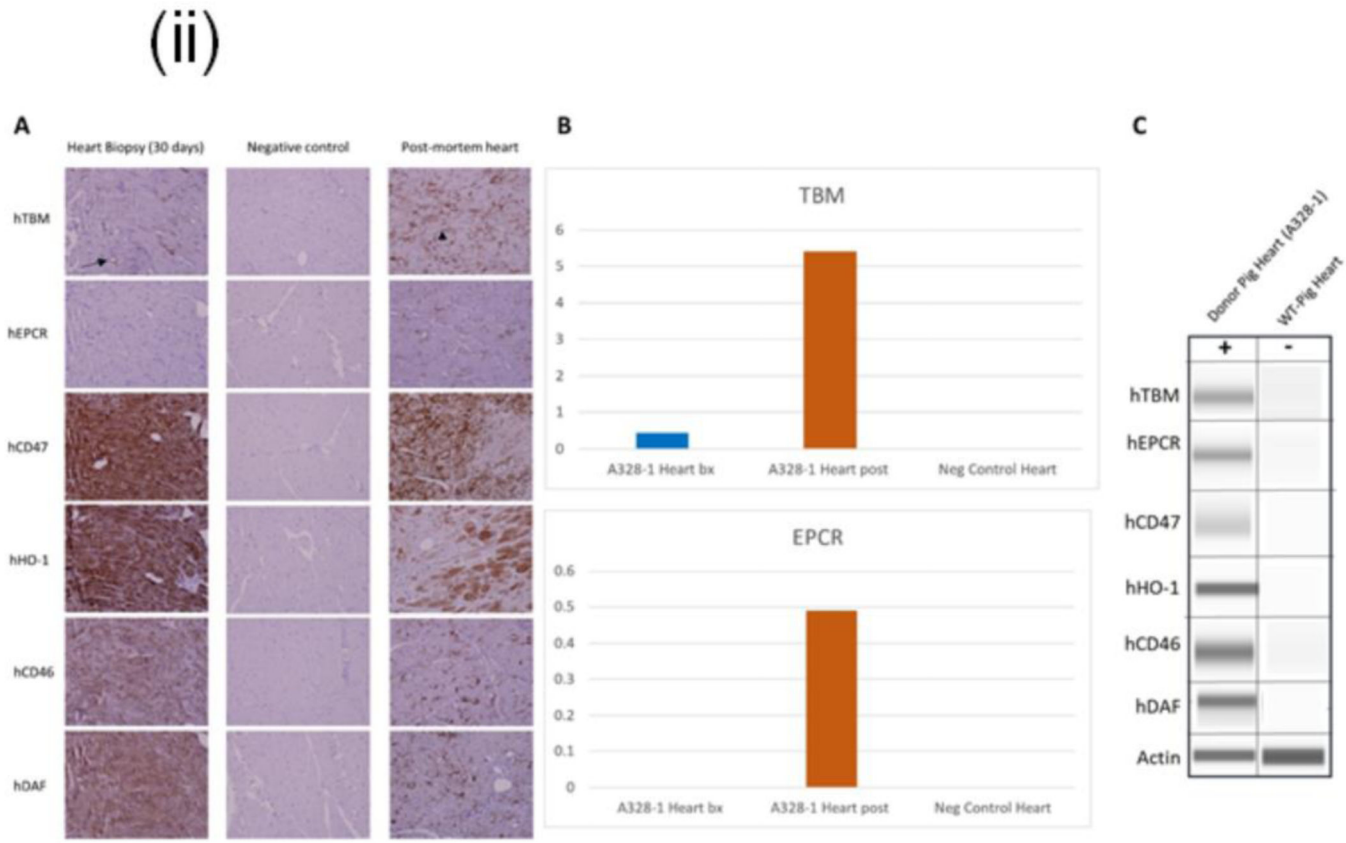

Figure 1.

(i): Phenotypic analysis of 10 gene edit pig(A328.1) and control quadruple knockout (QKO) and Wild type (WT) pig. A: Flow cytometric analysis of PBMCs to confirm deletion of Gal KO by the absence of IB4 lectin binding, CMAH KO by the absence of anti-Neu5GC antibody staining, and β4GalNT2 KO by the absence of DBA lectin staining, **B:** Western blot analysis of hTBM, hEPCR, hCD47, hHO1, hCD46, and hDAF transgene expression in the tail biopsy, and **C:** Serum IGF1 levels in donor and WT pig, reflecting GHR KO. **D.** Serological detection of anti-PCMV antibodies by western blot: PCMV glycoprotein B antigen (GenBank FJ595497.1; 2305–2574bp) was cloned, expressed and purified from an *E.Coli* 10X Histag vector (Origene). PCMV antigen was probed with pig sera or antibodies as described using western blot system (Simple Wes, Bio-techne) : His-tagged PCMV antigen was run on Lanes 1–6 in an automated capillary western; Lanes 1–3: A328.1 pig serum at increasing dilutions, and rabbit anti-pig IgG secondary antibody Lane 4: positive control (PCMV positive pig serum, and rabbit anti-pig IgG secondary antibody); Lane 5: negative control (PCMV anti-pig IgG secondary antibody alone (no serum); Lane 6: positive control (rabbit anti-His antibody and Mouse anti-Rabbit secondary antibody). Similar results were observed with PCMV glycoprotein B antigen (GenBank AF268039; 2771–31118bp). **E**. Quantitation of band densities in D (6x His tag positive control not shown). A328.1 anti-PCMV IgG was positive to a titer of 1:300. Similar results were observed with PCMV glycoprotein B antigen(GenBank AF268039; 2771–31118bp).

(ii): Transgene expression of endomyocardial biopsy (EMB) and xenograft after post-mortem. A: hTBM, hCD47, hHO1, hCD46, and hDAF were expressed at detectable levels in EMB and Xenograft along with negative control by IHC. hEPCR expression is below the level of detection in the Day 30 biopsy. hTBM expression is restricted to endothelial in the Day 30 biopsy (arrow) but upregulated in the post-mortem sample, a prudential indicator of stress, inflammation, or coagulation. Moreover, expression was detected in non-endothelial cell types in the xenograft after post-mortem (arrowhead), **B:** Relative IHC pixel density quantitation hTBM and hEPCR expression of the Day 30 heart biopsy compared to the post-mortem heart sample and **C:** Western blot analysis of transgene expression in xenograft after post-mortem. hTBM, hEPCR, hCD47, hHO1, hCD46, and hDAF are expressed at expected molecular weights.

i.

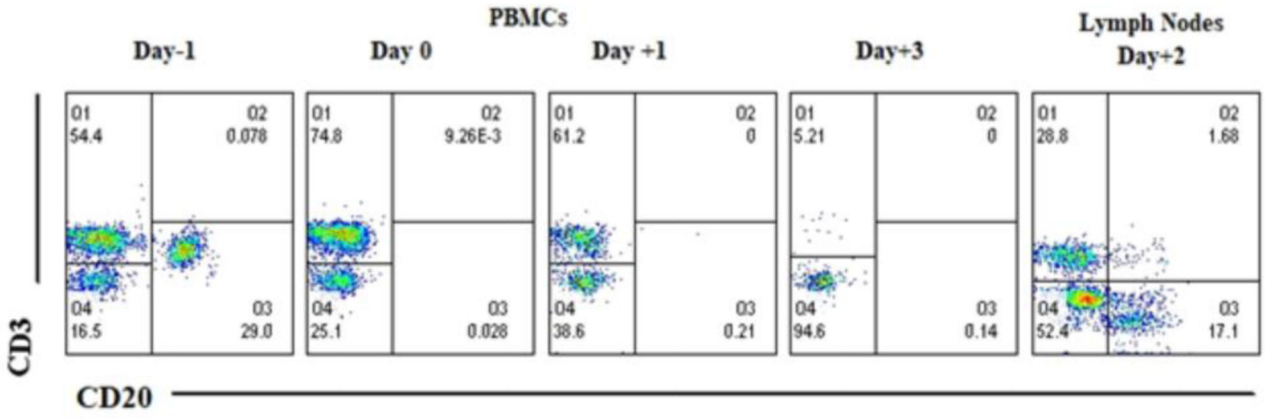

ii.

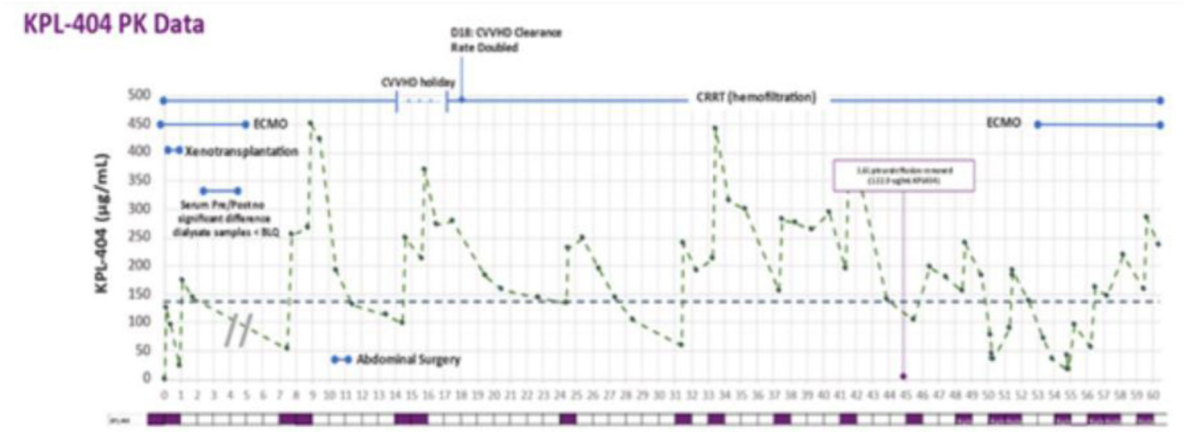

iii.

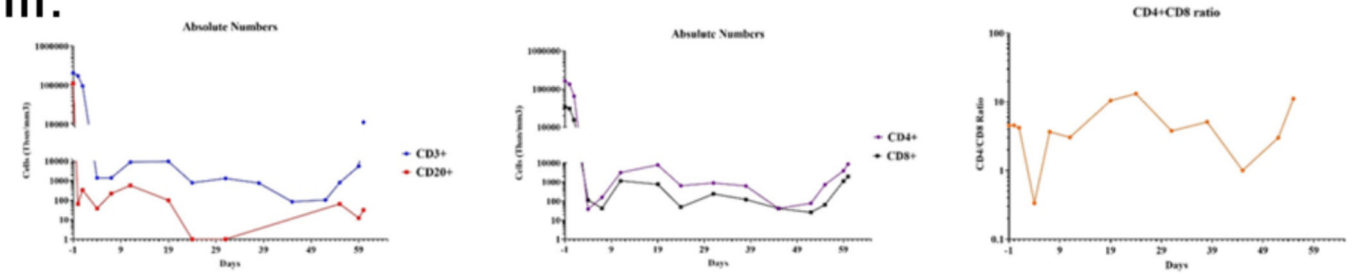

vi.

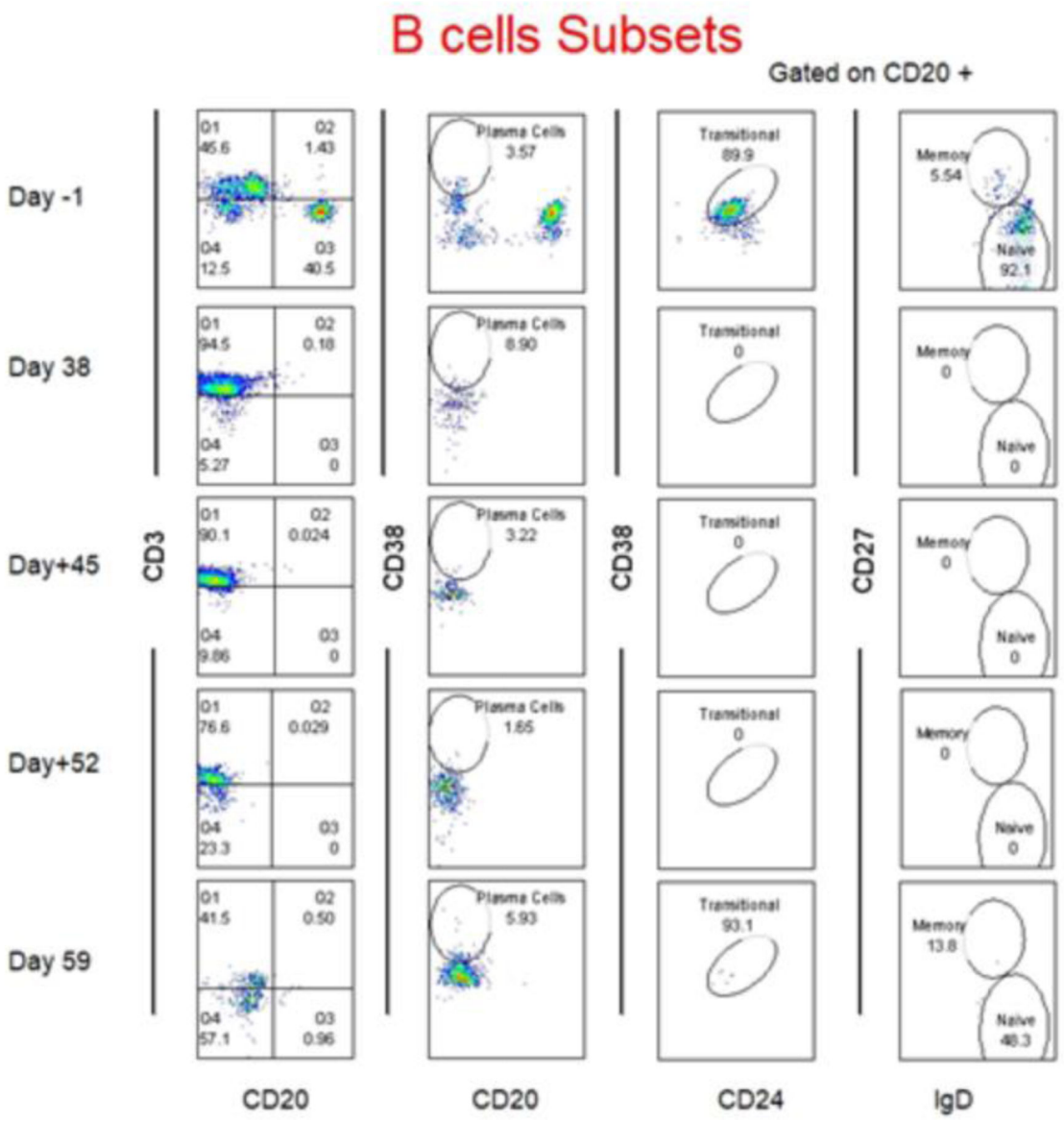

V.

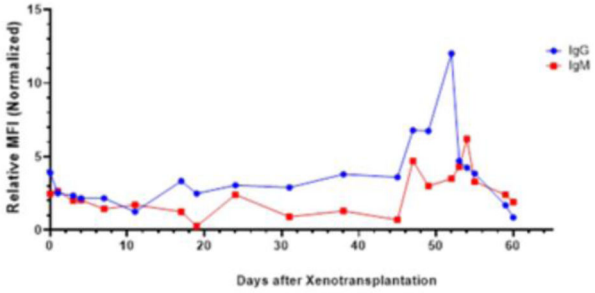

vi.

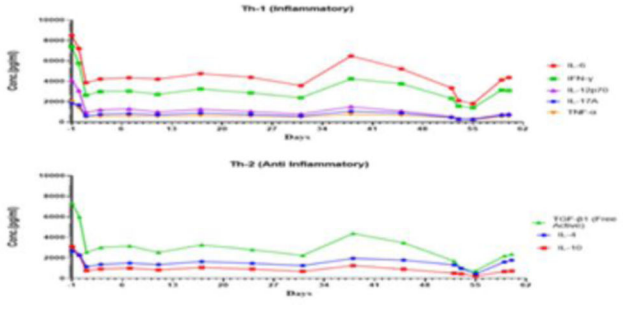

vii.

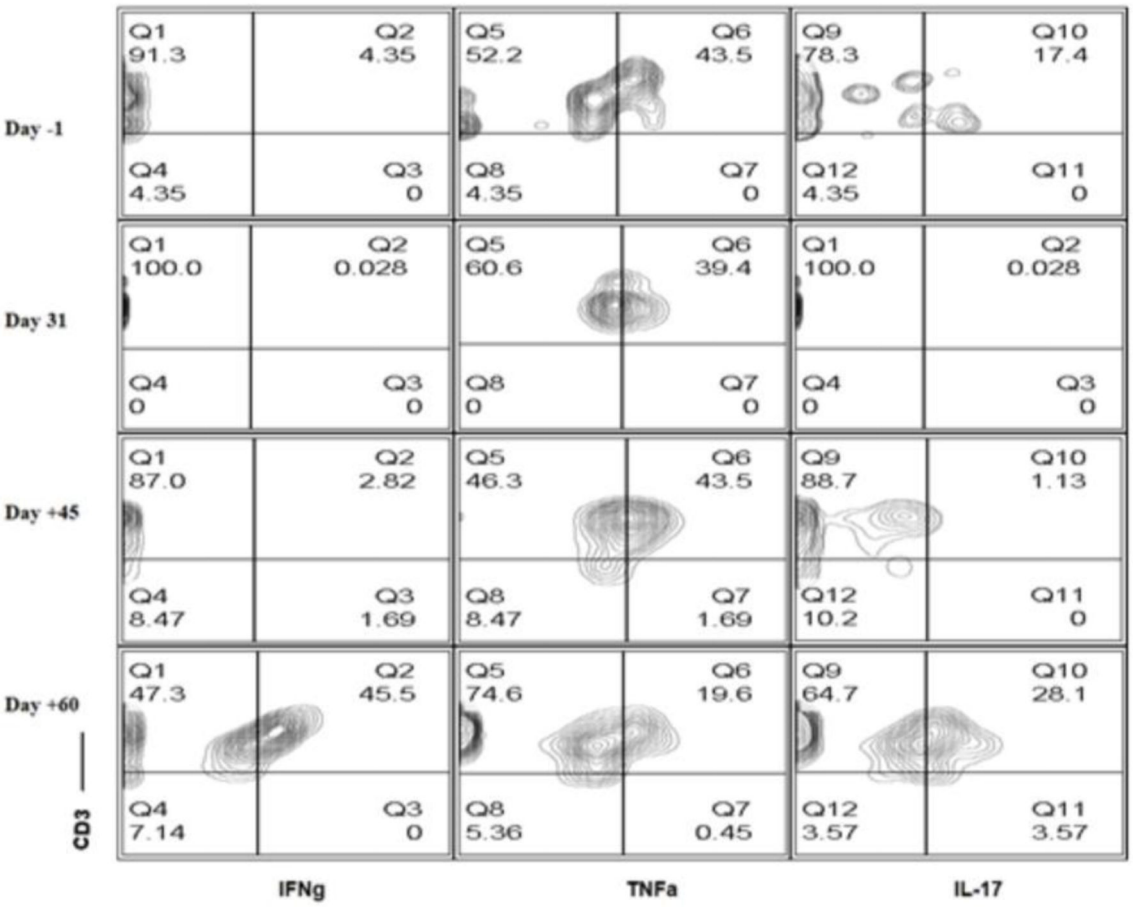

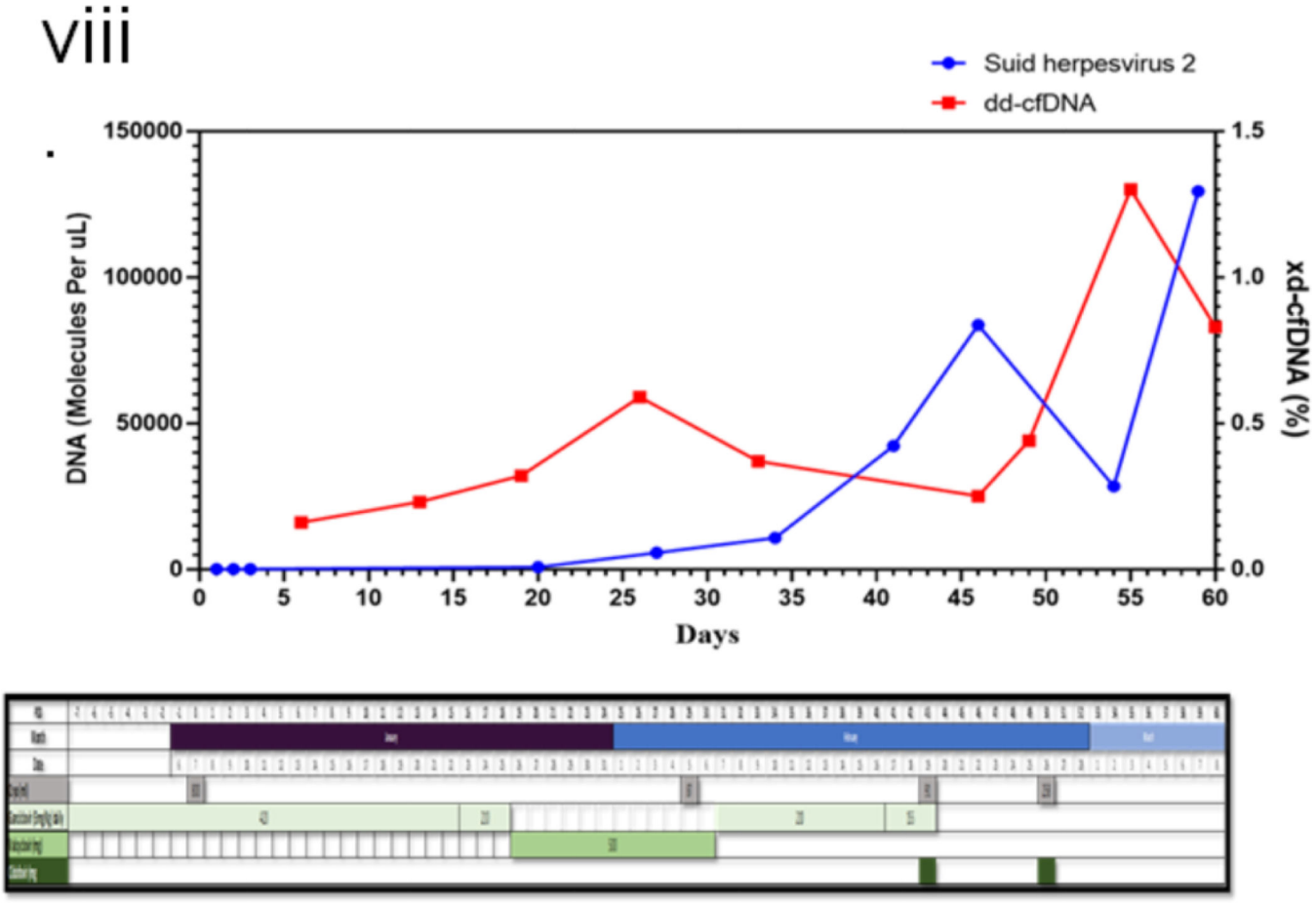

Figure 2: Immunosuppression and Immune monitoring of the recipient.

i: Flow cytometric analysis of the recipient's PBMCs (POD −1, 0,1, and 3) and lymph nodes (on day +2); **ii**: Relative PKA levels of KPL-404 administration at different time points (days).

iii: Absolute numbers of CD3+ & CD20+; CD4+& CD8+ and CD4/CD8 ratio; **iv**: Anti-pig non-Gal (IgG and IgM) antibodies titers, **v**: Serum cytokine levels; **iv**: Anti-viral therapy in relation to the detection of porcine cfDNA in patient's blood. Viral therapy was adjusted based on the patient's clinical condition or response to changes in the WBC count.

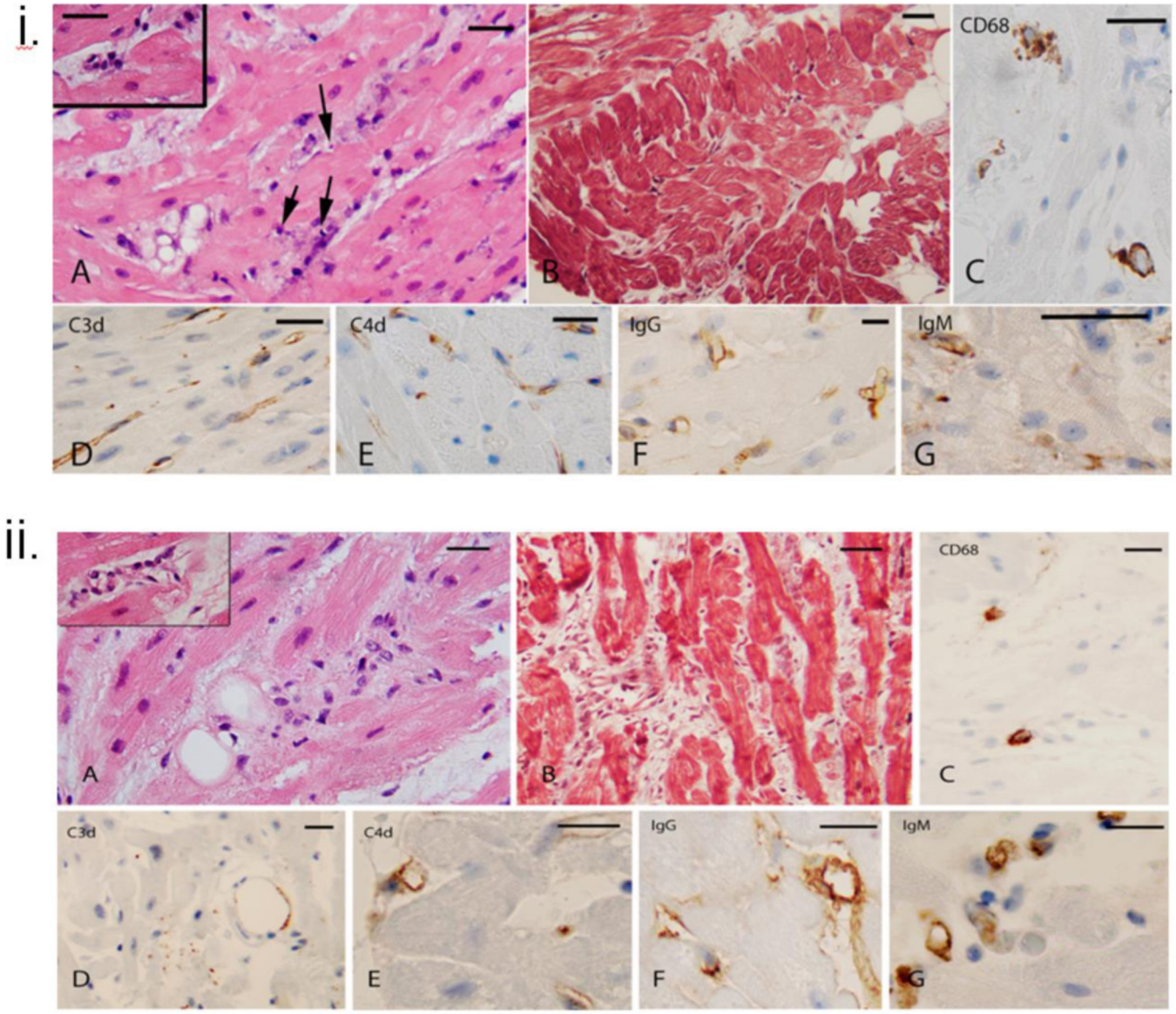

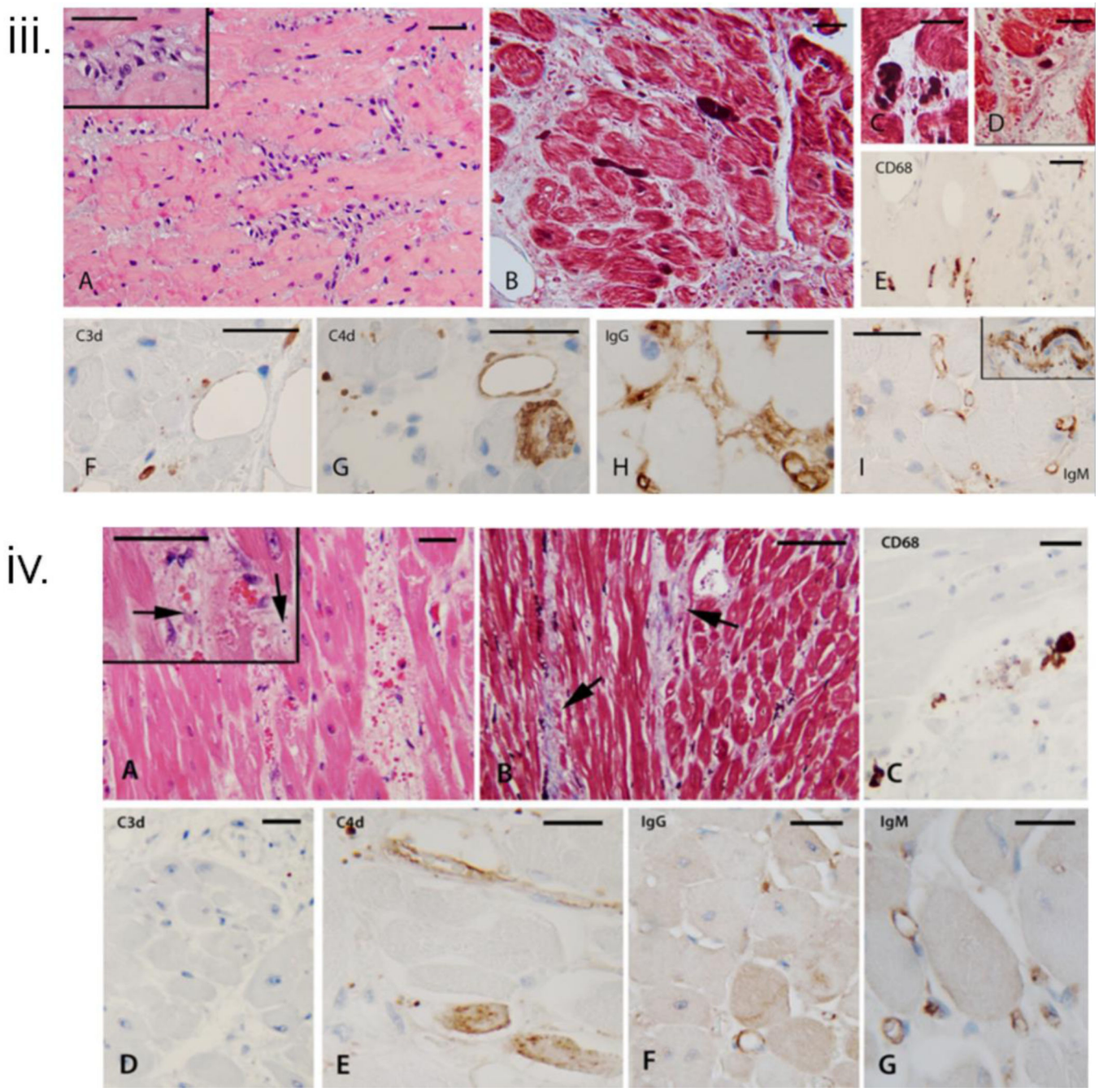

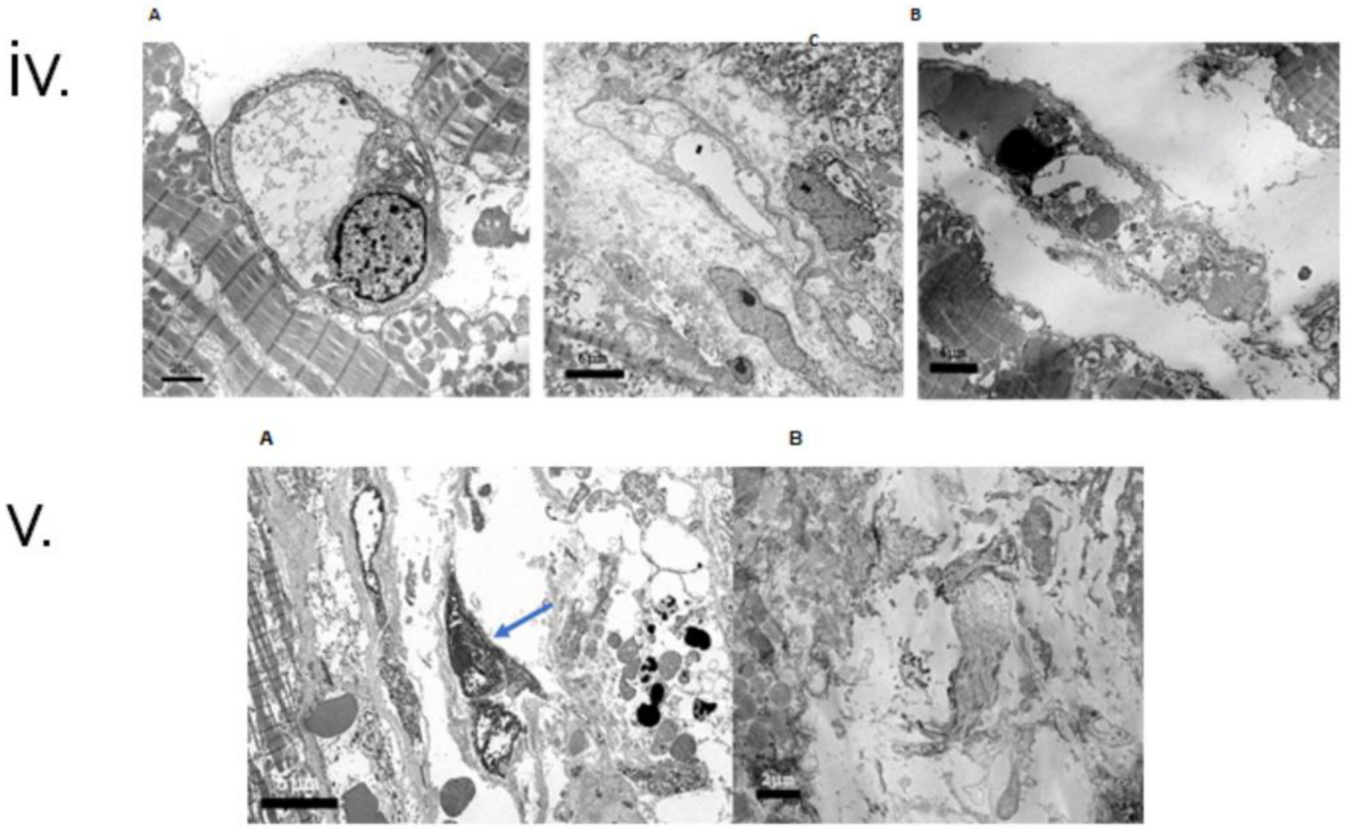

Figure 3.

i. Histopathology and immunohistochemistry of endomyocardial biopsy (EMB) on POD 34. A: On the H&E stain, there is mild interstitial edema in the myocardium with subtle injury of the endothelium with features suggestive of apoptosis (nuclear condensation and nuclear fragments (arrows). Insert cluster of enlarged endothelial cells in a slightly edematous interstitium, **B**: Trichrome stain to highlight interstitial collagen is within normal limits, **C**: CD68 stain demonstrates clusters of macrophages. The distribution in clusters suggests an intravascular location, **D, E, F**, and **G** demonstrate deposition in the C3d, C4d, IgG, and IgM microvasculature. Bars represent 50 microns.

ii. Histopathology and immunohistochemistry of endomyocardial biopsy (EMB) on POD 50. A: On the H&E stain, there is significant interstitial edema with a cluster of disorganized endothelium and mononuclear cells. Insert: Abnormal endothelial cells line the microvasculature, **B**: Trichrome stain highlights the separation of the myocardiocytes by expanded interstitium due to edema and an increase in spindle interstitial cells (fibroblasts), **C**: CD68 stain demonstrates occasional macrophages, **D**: CD3 stain shows insignificant punctate staining and outlines a fat globule. **E, F**, and **G** demonstrate C4d, IgG, and IgM microvasculature deposition. Bars represent 50 microns.

iii. Histopathology and immunohistochemistry of endomyocardial biopsy (EMB) on POD 59. A: On H&E stain, the interstitium is expanded by a mixed population of cells representing disorganized microvasculature and incipient interstitial fibrosis. Insert Higher magnification of the cellular areas, **B**: Trichrome stain confirms the presence of fibrous interstitial expansion with incipient collagenization. The interstitium has

abundant cell fragments and extravasated red cells in some areas. Thrombi are noted to appear as dark elongated structures, **C** and **D**: Trichrome stain highlights thrombi in the microvasculature, **D**: Trichrome stain demonstrates interstitial edema, incipient collagenization, and fragmented red cells, **E**: CD68 stain demonstrates rare macrophages that were noted predominantly in the subendocardial areas, **F**: C3d stain focally marks possible residual vascular spaces. **G:** C4d stain showed heterogeneous staining, focally, and **H** and **I** demonstrate the deposition of IgG and IgM in the microvasculature. Insert (top right) shows a thrombus highlighted by the IgM stain. Bars represent 50 microns

iv. Histopathology and immunohistochemistry of explanted cardiac xenograft at necropsy. A: H&E sections demonstrated edematous interstitial areas with abundant extravasated red blood cells. Insert: Arrows mark apoptotic nuclear fragments in the interstitium. In addition, not depicted in the images were single cell and confluent areas of myocyte necrosis, **B**: Trichrome stain highlighted incipient areas of collagen deposition in the expanded, edematous interstitium, **C**: The CD68 stain highlighted rare clusters of macrophages, **D**: The C3d stain was essentially negative, **E:** The C4d stain was overall negative, with the endothelium of rare arterioles decorated (top area). The lower parts of the image show isolated necrotic myocytes marked by the stain in a non-specific manner, **F:** IgG stain marks the outline of very rare microvascular spaces, and **G**: The IgM stain marks the outline of scattered capillaries.

v: Electron microscopy of endomyocardial biopsy (EMB) on POD 34 & 50. A: In the first biopsy on POD 34, More than 95% of arterioles were normal with quiescent endothelial cells. There was sparse interstitial tissue, and adjacent myocytes had normal myofilaments (M), **B**: In the first biopsy, exceptional capillaries had endothelial cell swelling. Note incipient interstitial expansion, edema, and degenerative features in the adjacent myocytes, **C:** Second biopsy on POD 50, more than 50% of capillaries had marked endothelial injury with cytoplasmic swelling, cell necrosis, and occasional apoptosis (arrow).

vi: Electron microscopy of endomyocardial biopsy (EMB) on POD 56 and explanted cardiac xenograft at necropsy. A: In the third biopsy on POD 56, severe endothelial injury and destruction were noted in most capillaries. Note enlarged nuclei (arrow), necrotic cellular fragments (arrowheads), and extravasated red cells (asterisks). Adjacent myocytes have swelling in myocytes and loss of myofilaments, and **B:** Cardiac xenograft after post-mortem demonstrates loss of capillaries in the interstitial space with early deposition of collagen bundles (fibrous organization, asterisk). Note loss of myofilaments in adjacent myocytes (M). Viral particles or viral cytopathic changes were not present in any sample.

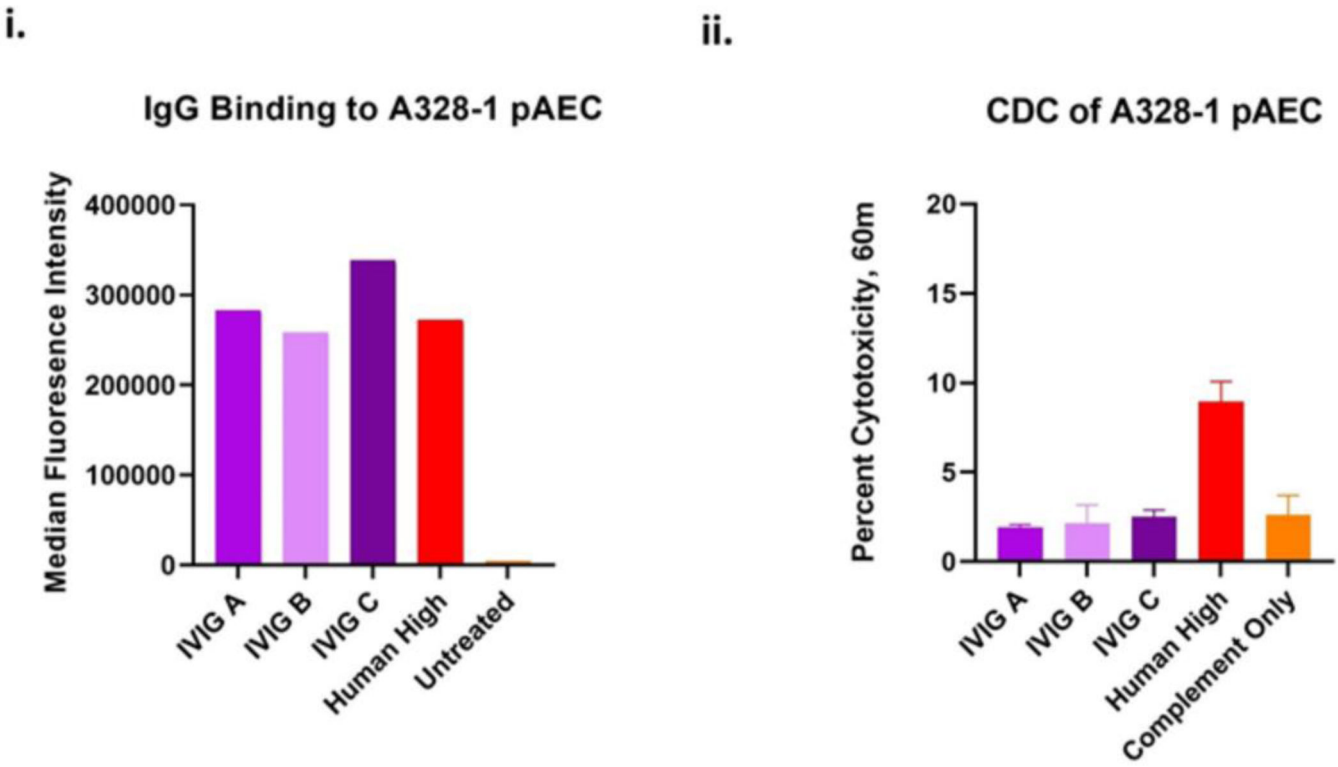

Figure 4: IVIG binding and cytotoxicity with PAECs:

A. IgG binding and **B** Cytotoxicity of IVIg: Three different lots of Gammagard IVIG (25mg/mL) and or 25% high control human sera binding to pig PAEC (A328–1).

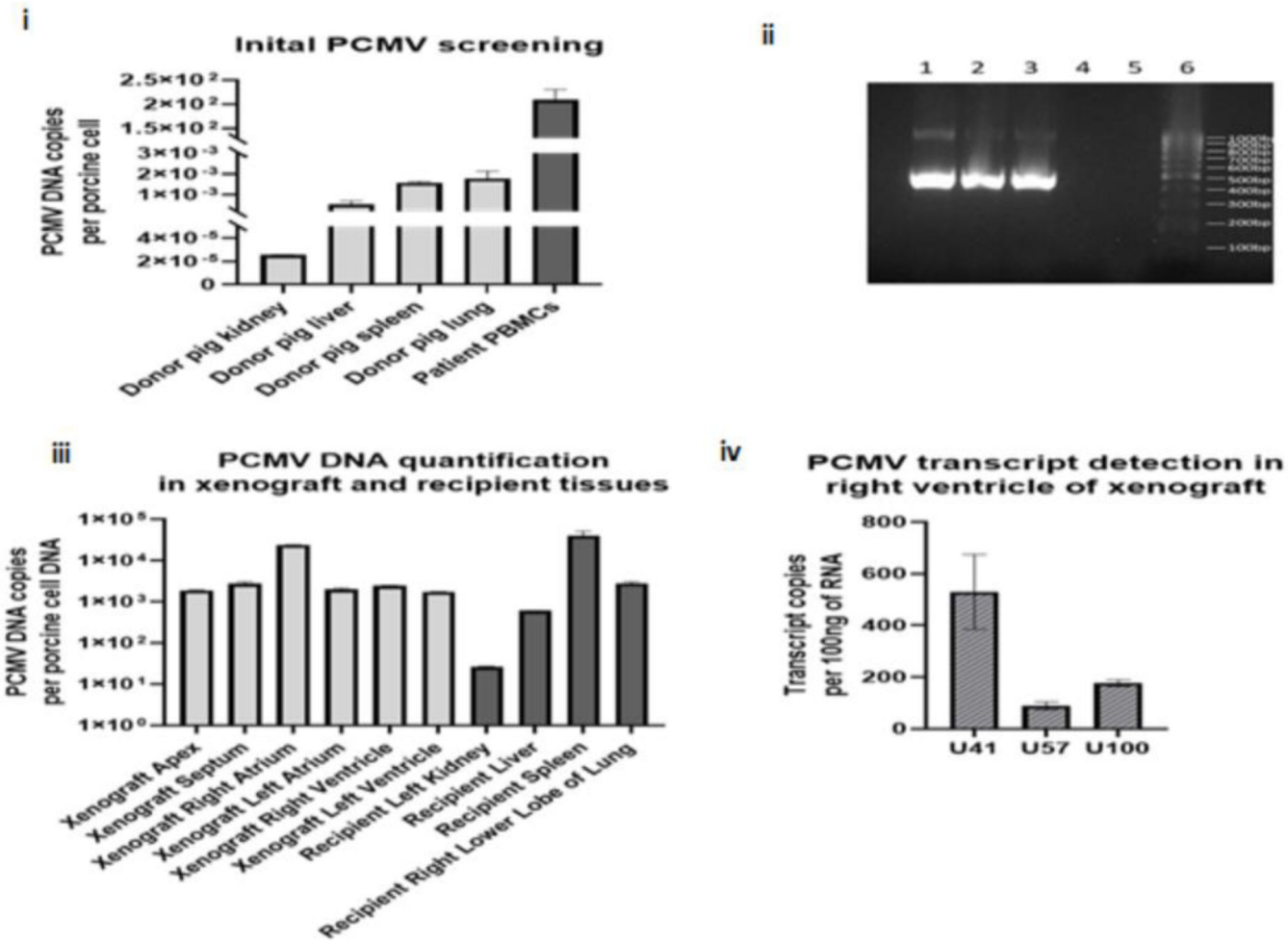

Figure 5: PCMV/PRV Investigations.

i: shows the PCMV/PRV DNA level detected in the pig tissue's initial screening from euthanasia and patient PBMCs from POD 45, as determined by qPCR normalized to one cellular load of porcine DNA, **ii:** confirmation of the initial PCMV/PRV investigation by conventional PCR for PCMV/PRV DNA, following electrophoresis on a 1.5% agarose gel. Lane 1: patient PBMCs, lane 2: pig spleen, lane 3: positive control, lane 4: negative control, lane 5: empty, lane 6: 100bp ladder, **iii:** PCMV/PRV DNA level detected in the xenograft compartments and recipient organs at autopsy; as determined by qPCR, PCMV/PRV DNA levels are normalized to one cellular load of porcine DNA, and **iv:** PCMV/PRV RNA transcripts detected within the right ventricle of the xenograft at autopsy, as determined by qRT-PCR. Transcript copies are normalized to 100ng of total RNA.

i.

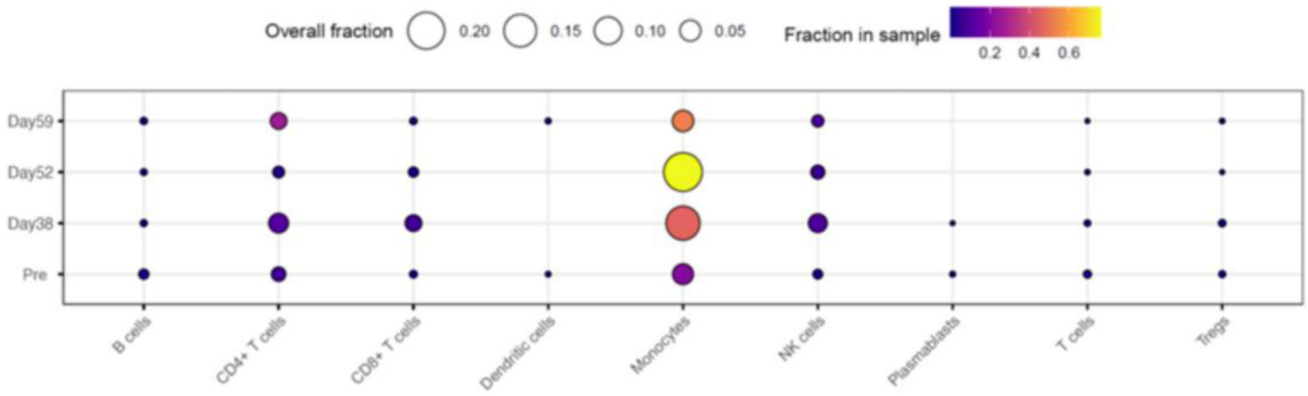

ii.

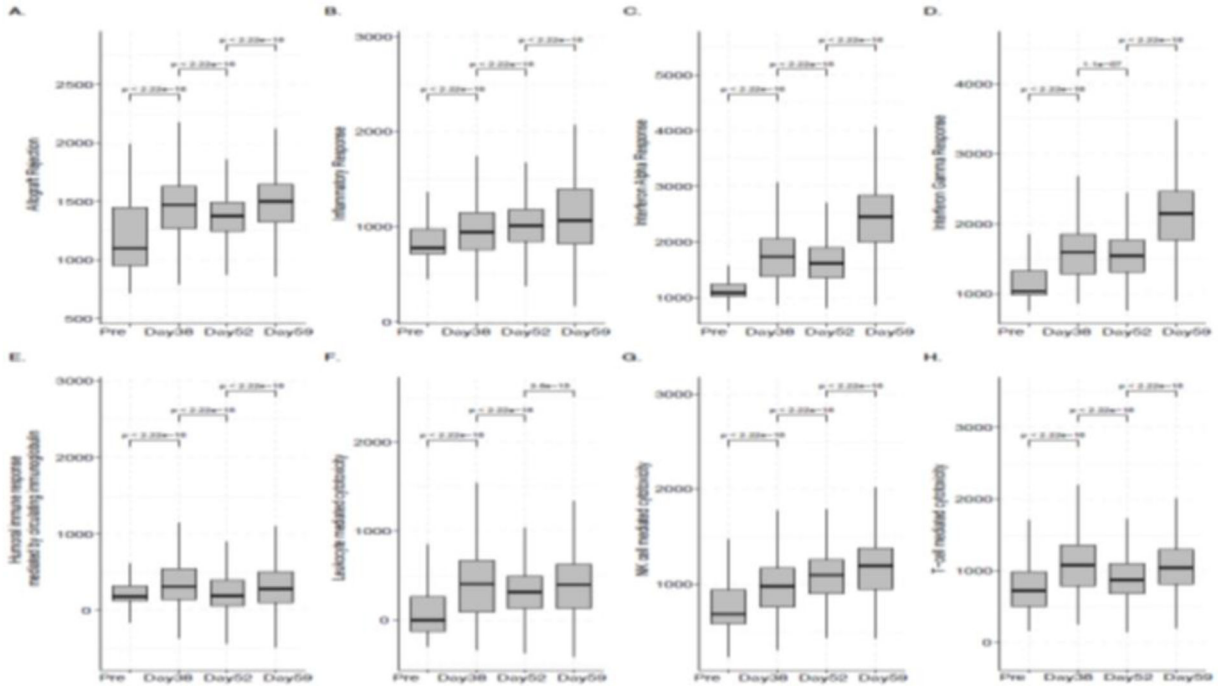

iii.

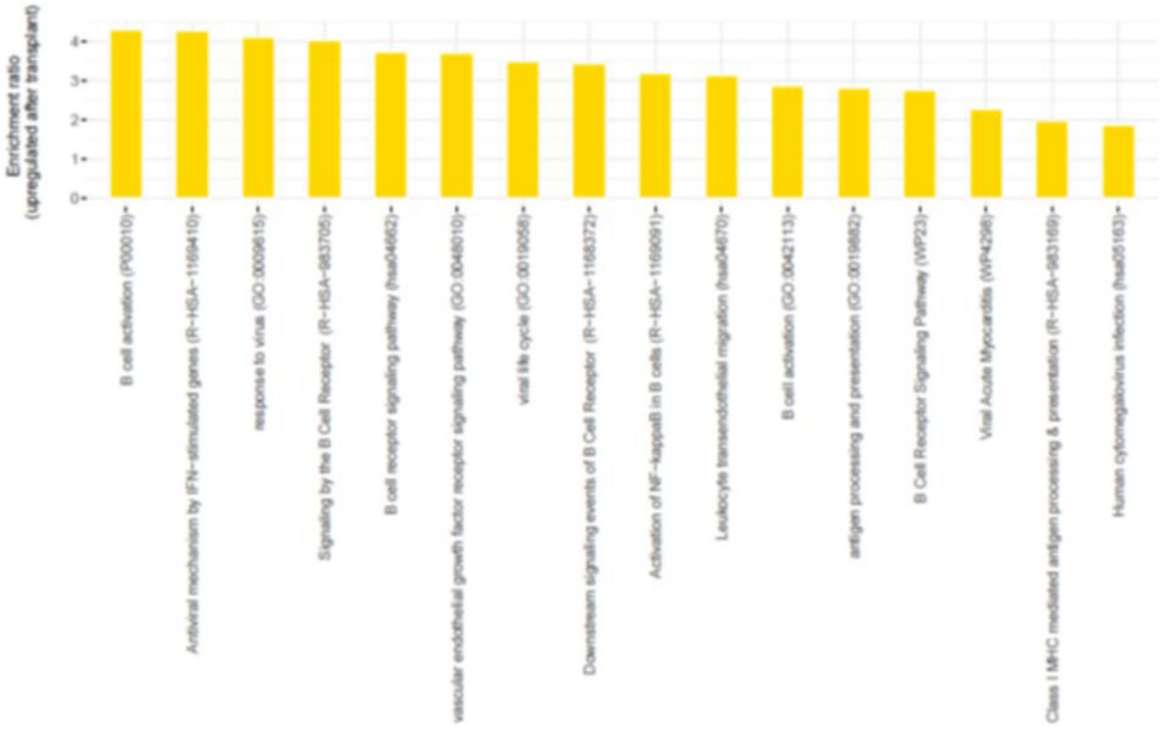

Figure 6: Single-cell RNA sequence analysis:

i. Changes in the immune cell type composition over time: Proportions of the major immune cell types in the integrated data set and at the sample level, where each sample corresponds to a different time point. The circle size and color correspond to each cell type's overall and time point-specific proportions, respectively. **ii. ssGSEA-based enrichment scores of relevant hallmark signatures:** Box plots showing the distributions (across all cells for each sample) of the hallmark gene set enrichment scores associated with (A) allograft rejection, (B) global inflammatory response, (C) interferon alpha, (D) interferon gamma-specific responses, (E) humoral immune response mediated by circulating immunoglobulin and in addition to cytotoxicity mediated by (F) leukocytes and specifically, by (G) NK cells and (H) T-cells. Each box plot shows the median and lower/upper quartiles as solid horizontal lines; whiskers extend to minima (lower quartile-1.5*interquartile range) and maxima (upper quartile+1.5*interquartile range), excluding the outliers. The reported p-values are computed from the pairwise comparisons of consecutive time points using the Wilcoxon rank sum test; **iii. Enrichment profile associated with BCR signaling, viral infection, and endothelial damage**. The enrichment ratios of the GO term and pathways (p-value<0.05) associated with the genes upregulated by at least 50% (with FDR~0) in the post-transplant samples compared to the pre-transplant sample.

Table 1.

Immunosuppression Regimen used